



UNIVERSITÀ
DEGLI STUDI
DI PADOVA

Exploration of X-ray Absorption Spectroscopy (XAS) in Catalysis

Ph.D. course “Elements of X-ray Physics” : 11-06-2024



Namratha Wooluvarana Naveenkumar
PhD student

- How XAS came into being?
- XAS Principle
- XANES & EXAFS -*Three distinct features in XAS spectra; EXAFS equation.*
- XAS measurement -*Experimental modes;*
- Time resolved XAS- *MEMS & capillary reactors*
- Case studies
 1. Incomplete formation of bimetallic alloy- Difference approach
 2. Importance of catalyst preparation protocol-XAS-CT.

How XAS came into being?

1913



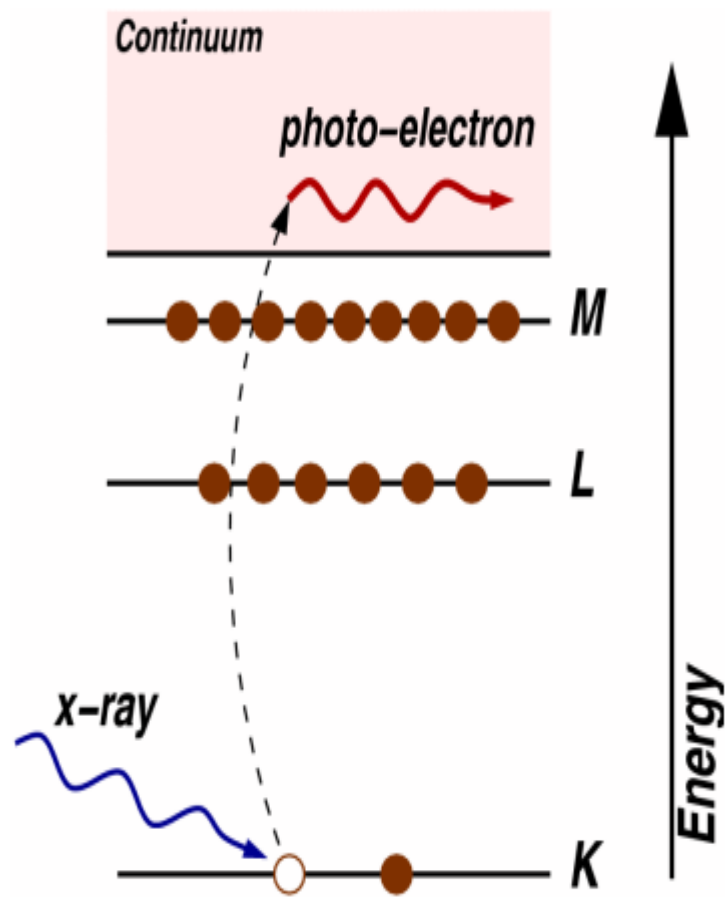
Maurice de Broglie

Table: EXAFS Family Tree.

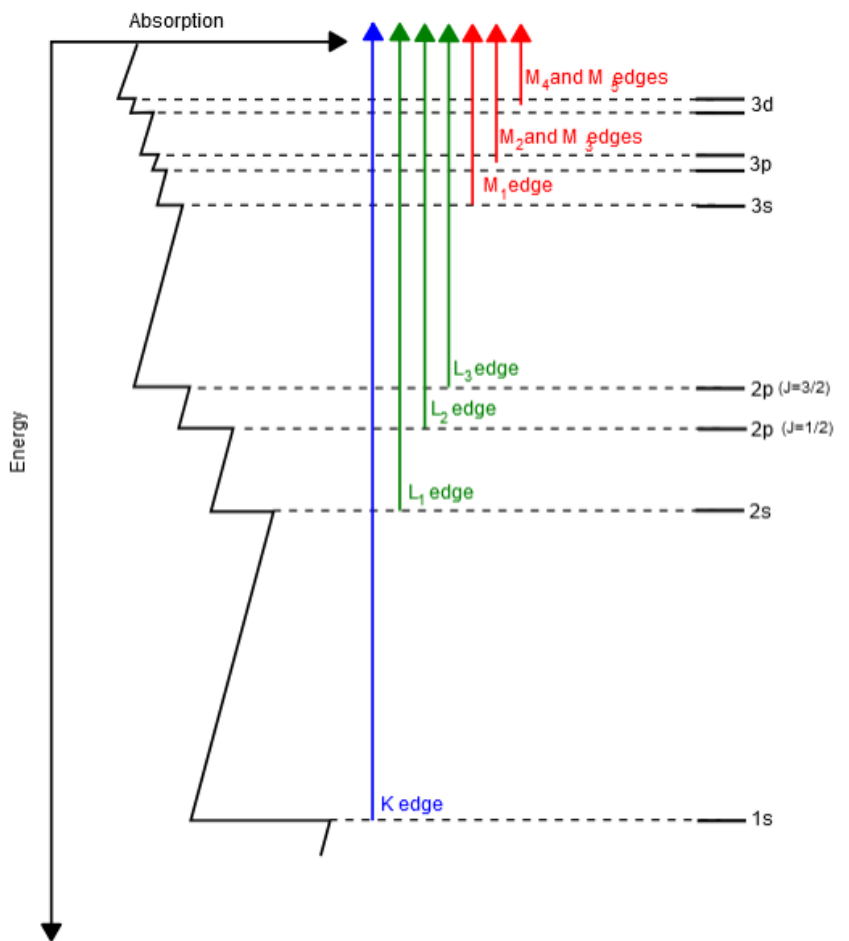
Röntgen (1895)	Discovered X-rays
Maurice de Broglie (1913)	Measured first absorption edge
World War I (1914–1918)	
Fricke (1920)	Observed first fine structure
Kossel (1920)	First theory of XANES
Hanawalt (1931)	EXAFS in gases, temperature effect
Kronig (1931)	First theory of EXAFS
Cauchois (1932)	Curved crystal transmission spectrograph
Hayasi (1936, 1949)	
Theory of EXAFS	
World War II (1941–1945)	
Sawada (1955)	Amorphous/crystalline polymorphs
Shiraiwa (1958)	Improved theory
Kostarev (1939, 1946)	Theory and measured EXAFS in single crystals
Kozlenkov (1960)	Improved theory
Van Nordstrand (1960)	Instrumentation, fingerprint ID, used XAS to characterize catalysts
Lytle (14 July 1960)	Starts work at Boeing (BSRL)
Krogstad (1960)	Personal communication
Lytle (1962)	Particle-in-a-box model
Prins (1964)	Helped name EXAFS
Parratt (1965)	Personal communication; <i>Rev. Mod. Phys.</i> (1959). 31 , 616
Sayers, Stern, Lytle (1968–1971)	Modern theory, Fourier transform of EXAFS
Sayers, Stern, Lytle (1974)	First trip to synchrotron (SSRL)



XAS Principle



The photoelectric effect, in which an x-ray is absorbed and a core level electron is promoted out of the atom. (1)



Transitions that contribute to XAS edges. (2)

EXAFS and XANES

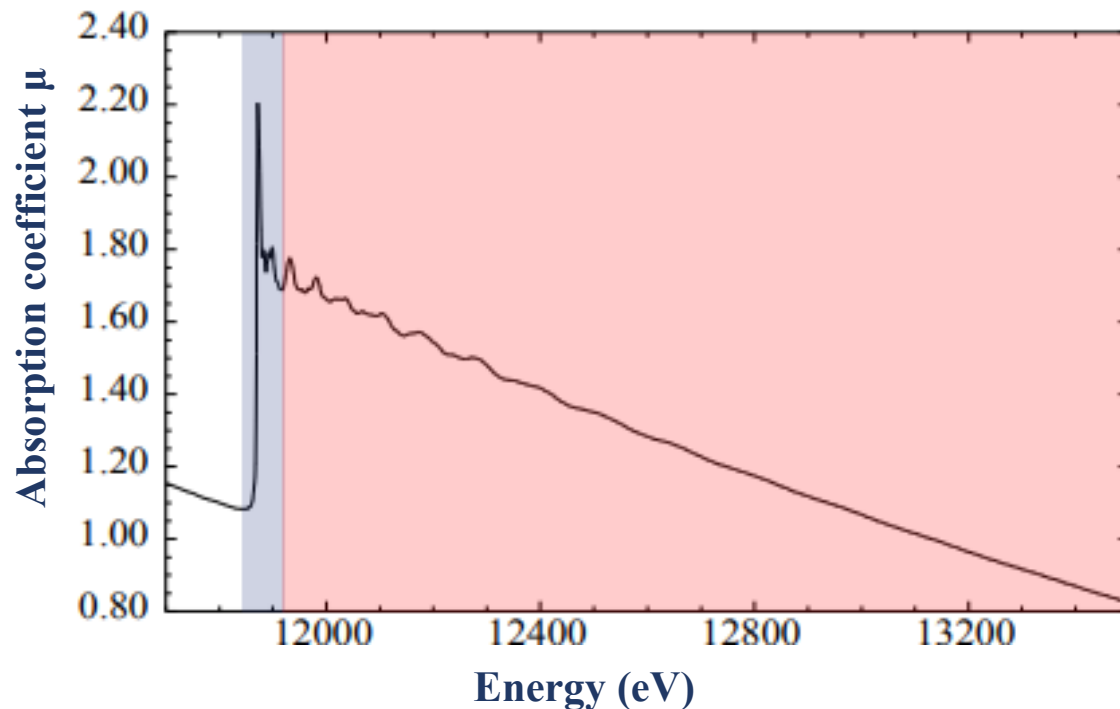
X-ray Absorption Spectroscopy (XAS) is divided into 2 regimes:

XANES: X-ray Absorption Near-Edge Spectroscopy

EXAFS : Extended X-ray Absorption Fine-Structure

XANES : transitions to unfilled bound states, nearly bound states, continuum - **low energy photoelectrons**

EXAFS: ~ 50 – 1000 eV from edge, transitions to continuum – **high energy photoelectrons**

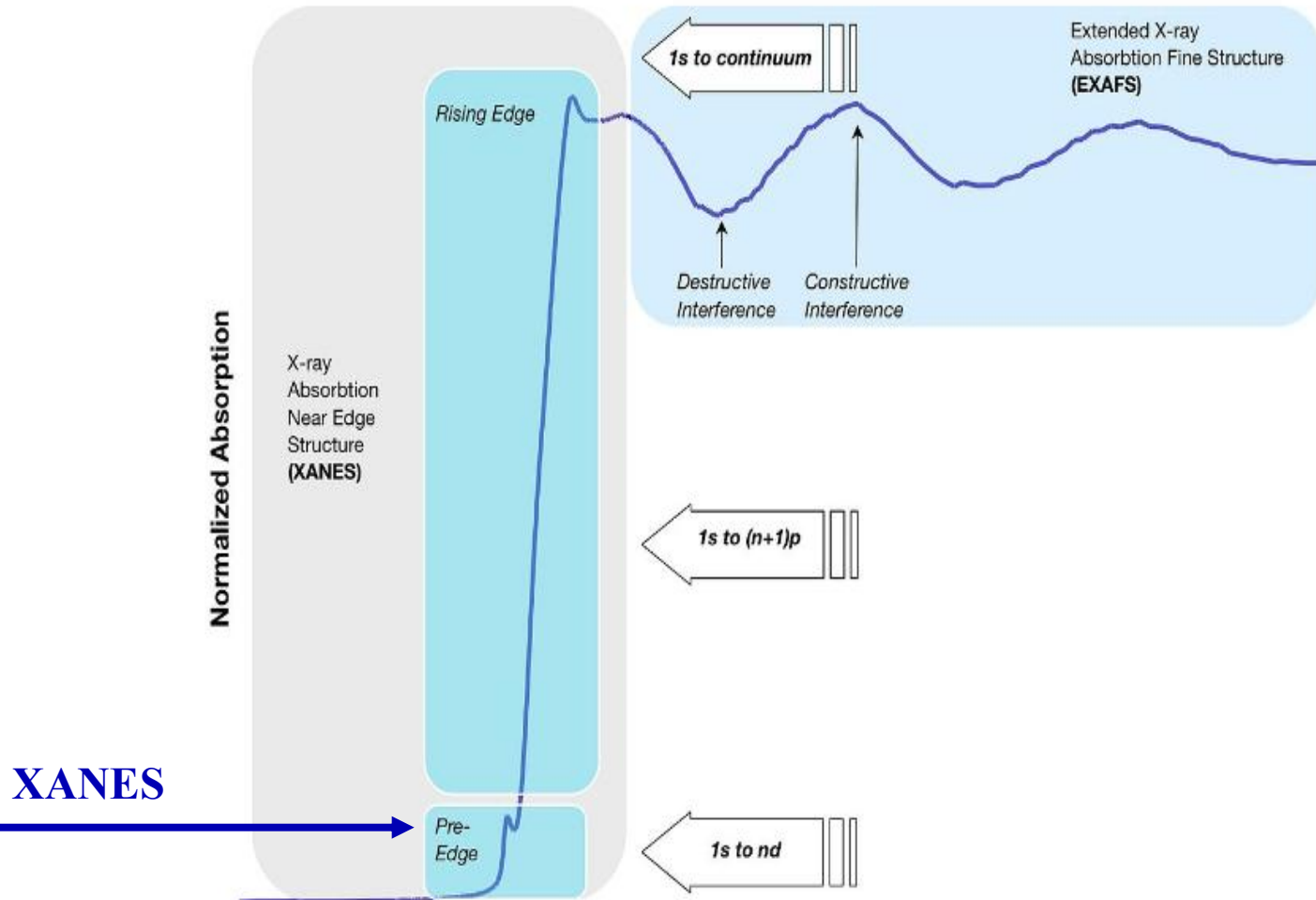


Example of XAS spectrum

Three major events – distinct features



1. Pre-edge
The threshold of absorption which is distinct for excitations into the lowest unoccupied states.



Example XAS spectrum showing the three major data regions.

Three major events – distinct features

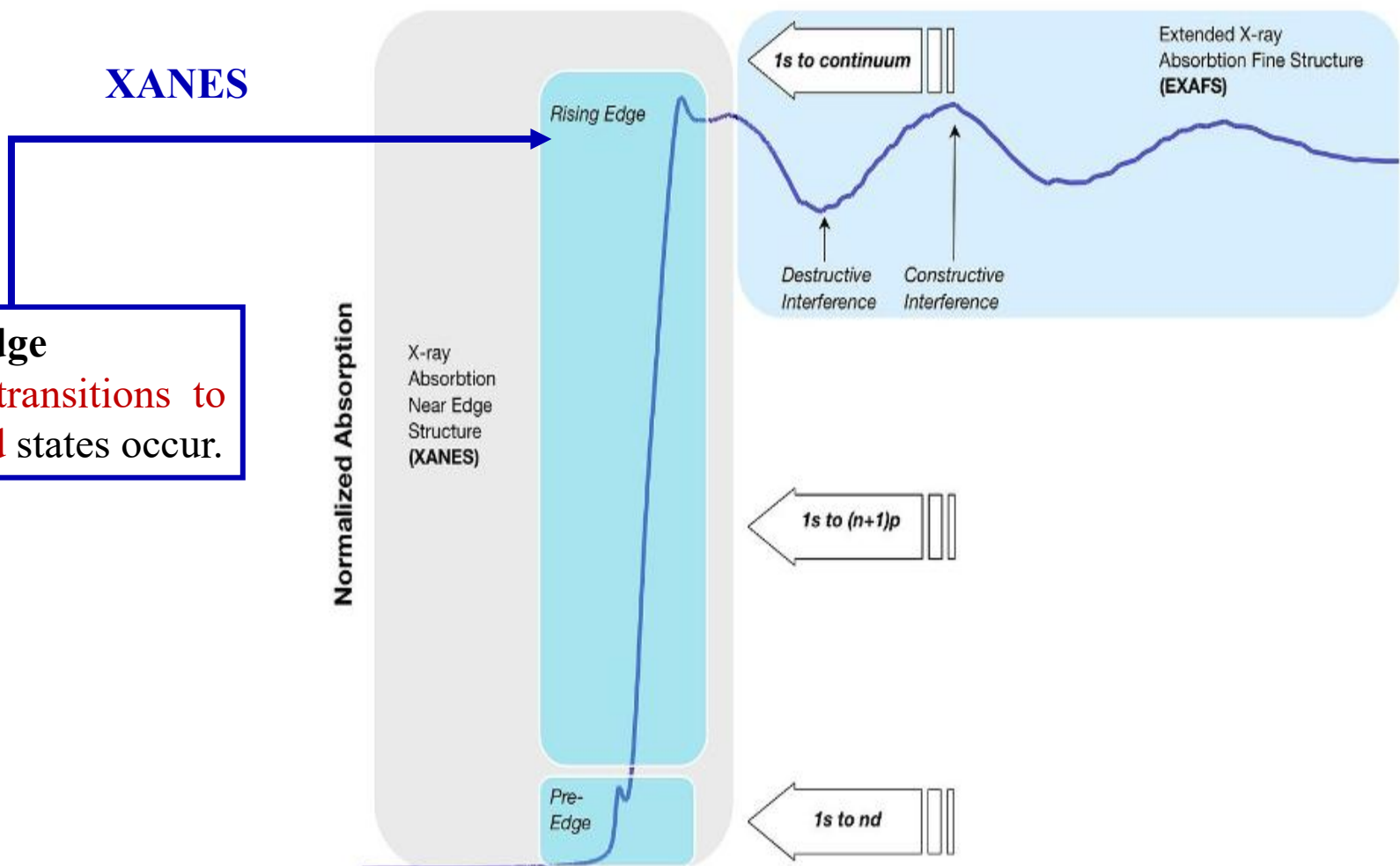
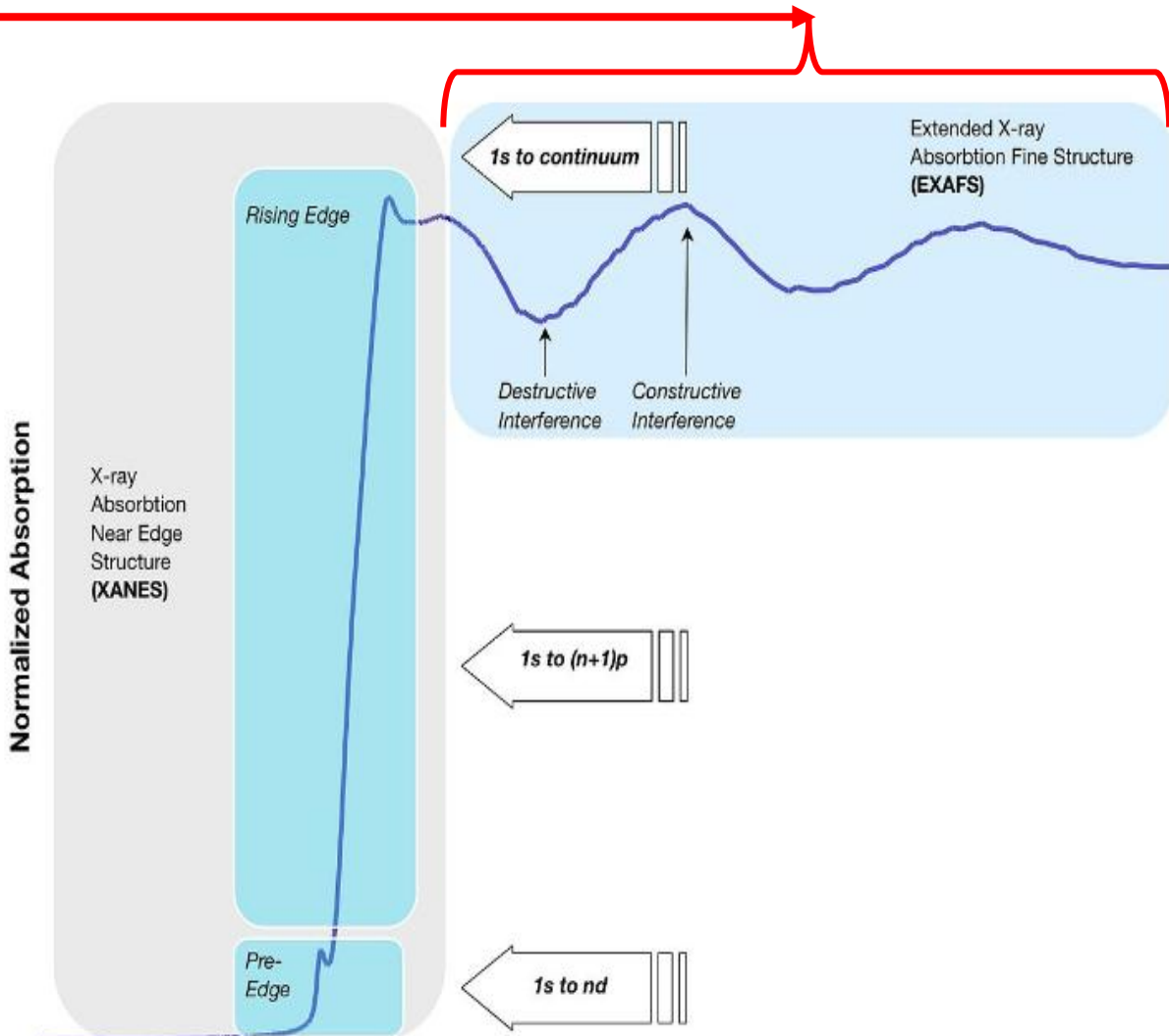


Figure : Example XAS spectrum showing the three major data regions.

Three major events – distinct features

EXAFS

3.Scattering of electrons with neighboring atoms. In the high-kinetic-energy range, the **constructive and destructive interference** of the resonance of excited electrons at fixed positions of neighboring atoms gives rise to clearly distinguishable absorption features (oscillations).



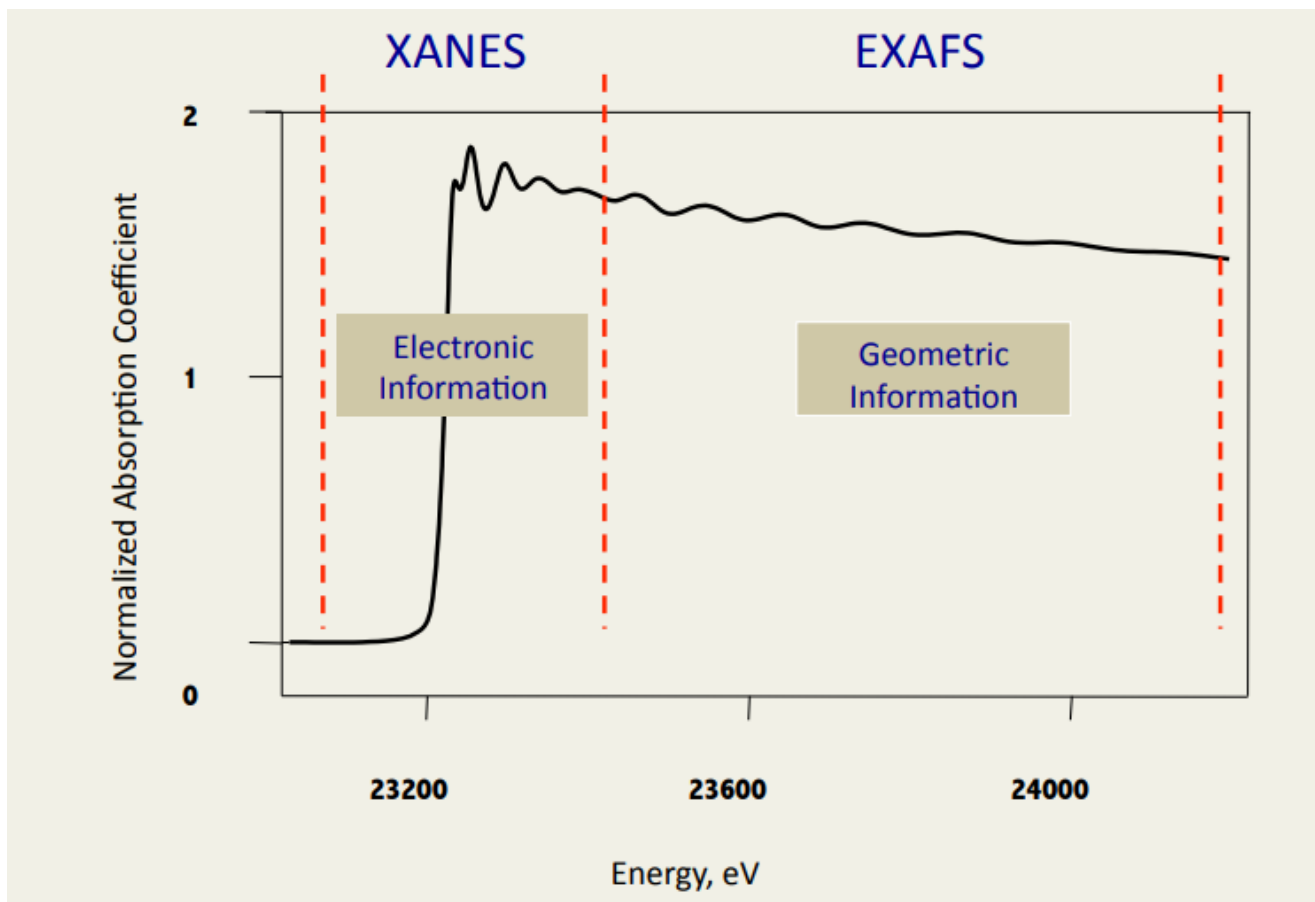
Example XAS spectrum showing the three major data regions.

EXAFS and XANES



XANES-estimations of ligand fields, spin states, or the charge on a metal carrier (oxidation state).

EXAFS- Identity, Coordination number (N), Interatomic distances (R) of backscattering atoms.



Example of XAS spectrum

The EXAFS Equation

$$\chi(k) = \sum_j \frac{N_j S_0^2 f_j(k) e^{-2R_j/\lambda(k)}}{k R_j^2} e^{-2k^2 \sigma_j^2} \sin[2kR_j + \delta_j(k)]$$

Amplitude reduction term
Photo-electron mean-free path (including core-hole lifetime)
Thermal and static mean-square disorder in R

If we know the **scattering** properties of the neighboring atom: $f(k)$ and $\delta(k)$, and the mean-free-path $\lambda(k)$ we can determine:

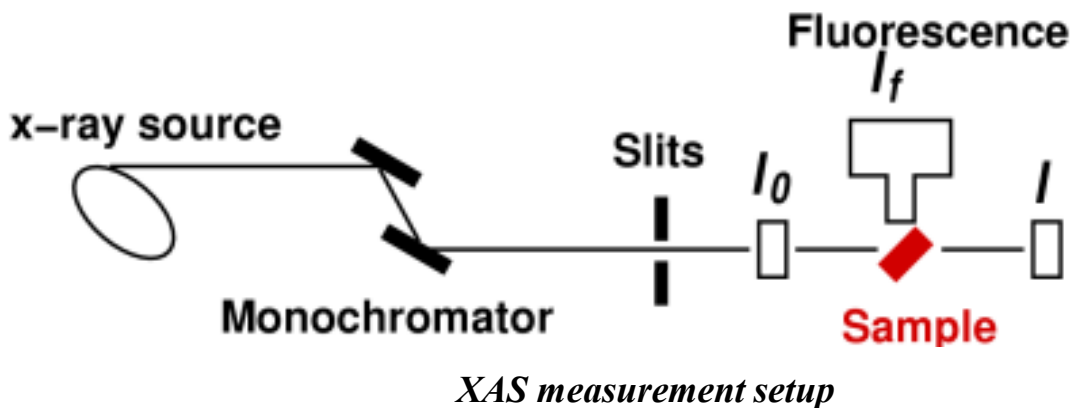
R distance to neighboring atom.

N coordination number of neighboring atom.

σ^2 mean-square disorder of neighbor distance.

The scattering amplitude $f(k)$ and phase-shift $\delta(k)$ depend on **atomic number**, so that XAFS is also sensitive to **Z** of the neighboring atom

X-ray Absorption measurements



XAS measures the energy dependence of the **x-ray absorption coefficient $\mu(E)$** at and above the absorption edge of a selected element.

$\mu(E)$ can be measured in two ways:

Transmission:

$$\begin{aligned} I &= I_0 e^{-\mu(E)t} \\ \mu(E)t &= -\ln(I/I_0) \end{aligned}$$

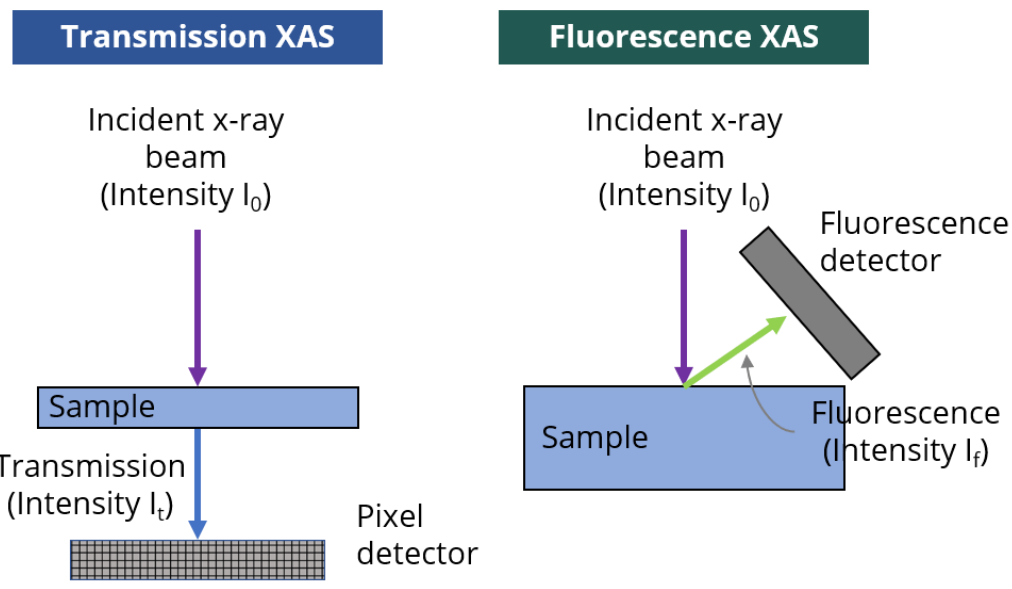
Fluorescence:

$$\mu(E) \propto I_f / I_0$$

Choosing the Correct Experimental Mode

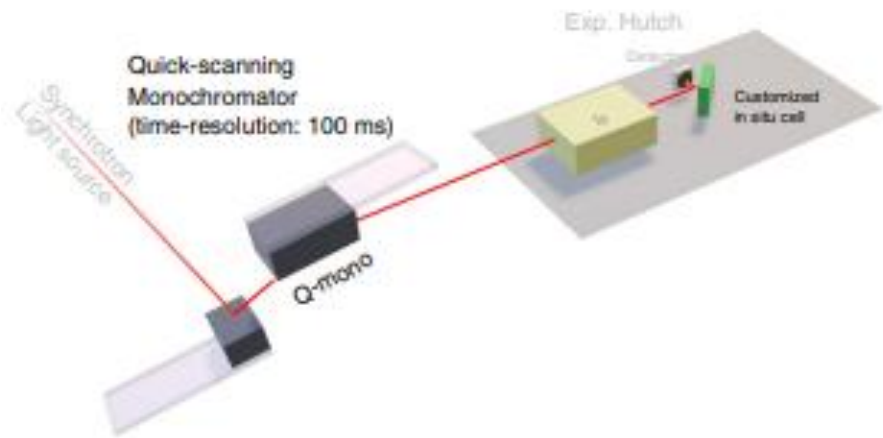


- **Choosing the right Measurement Mode:** Transmission or Fluorescence
- **Key Considerations:** element of interest, its absorption edge energies, its concentration and distribution, and the physical state of the sample.
- **Transmission Experiments:** pass through straight line-Sample uniformity- *Rule of thumb* ~ 4 absorption lengths.
- **Fluorescence Mode:** concentration of the element of interest - emission is detected-detector is placed at an angle.
- **Detector Placement:** to *maximize emission yield and minimize noise from scattering*.

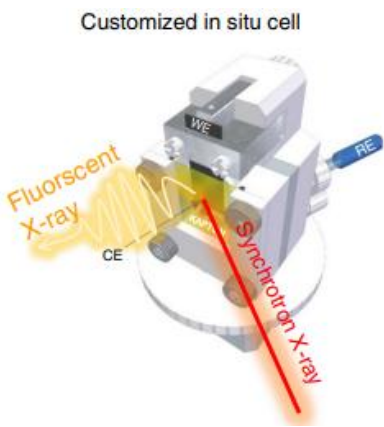


Experimental modes in XAS

Time resolved X-ray absorption spectroscopy (XAS)

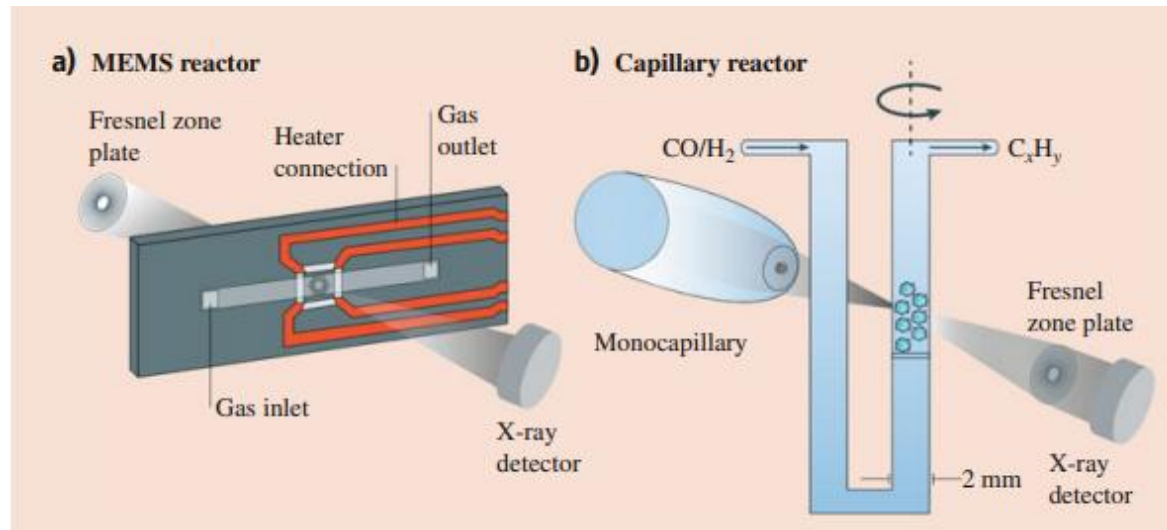


The schematic diagram of the setup of operando time-resolved XAS experiments



Representation of customized operando XAS cell.

MEMS & Capillary reactor



Two reactor designs used for time-resolved long-duration in situ or operando

Microelectromechanical system reactor

- Experiments using **soft** XAS.
- Both for liquid and solid studies(the attenuation length < total absorption).

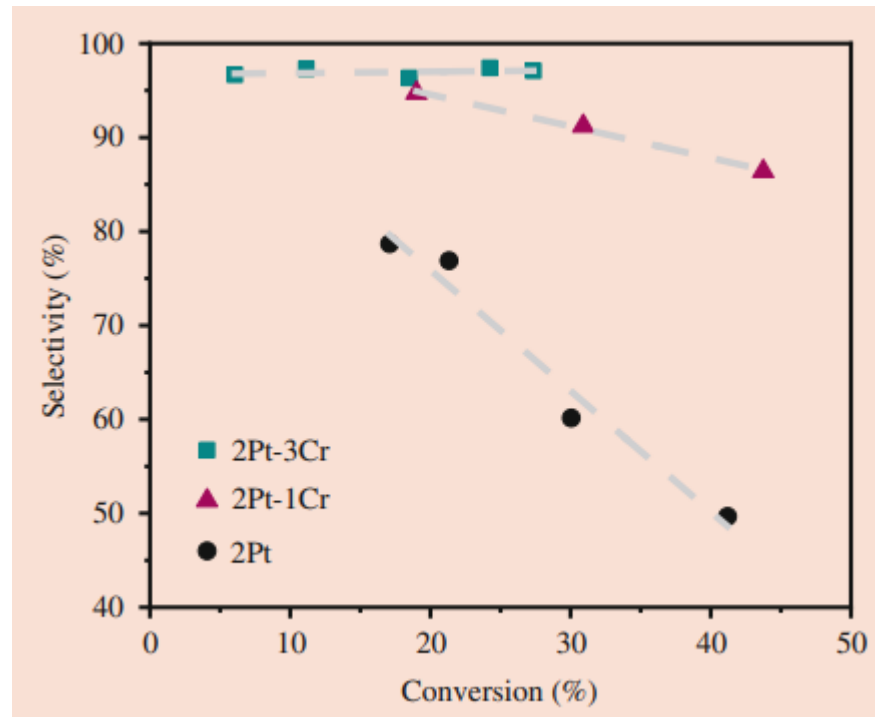
Capillary reactor

- Solid catalysts using **hard** XAS .
- Operando studies choose **heterogeneous catalyst powders** reacting mainly with gases.

Case Study 1: Incomplete Formation of a Pt₃Cr Alloy

- Bimetallic catalysts of Pt-Cr-**propane dehydrogenation**, achieving propylene selectivity greater than 95%, which is superior to monometallic Pt nanoparticles.
- Preparation- incipient wetness impregnation method.

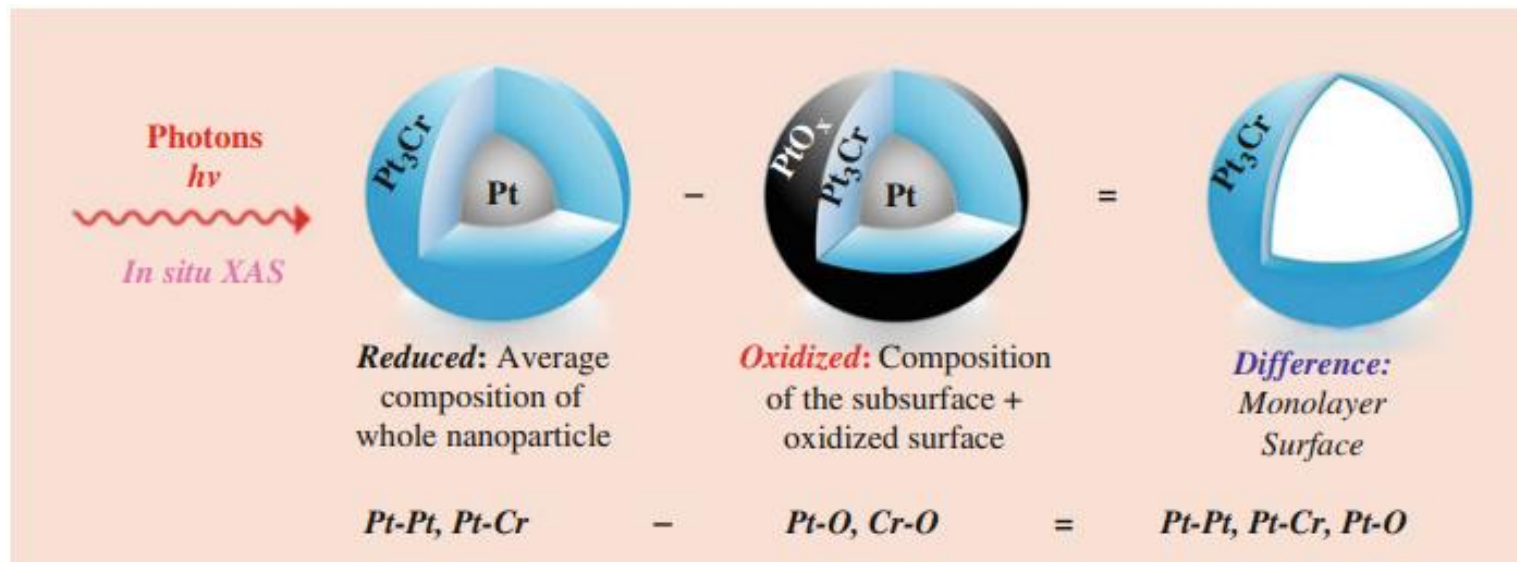
Catalysts	Denotation	Selectivity (%)	Particle size
2%Pt/SiO ₂	2Pt	75	
2%Pt-1%Cr/ SiO ₂	2Pt-1Cr	95	
2%Pt-3%Cr/ SiO ₂	2Pt-3Cr	98	~2 nm by STEM.



Propylene selectivity as a function of propane dehydrogenation conversion at 550 °C, 2.5% C₃H₈ and 2.5% H₂.

Why it is necessary to determine the surface structure and how this can be determined using the surface EXAFS analysis?

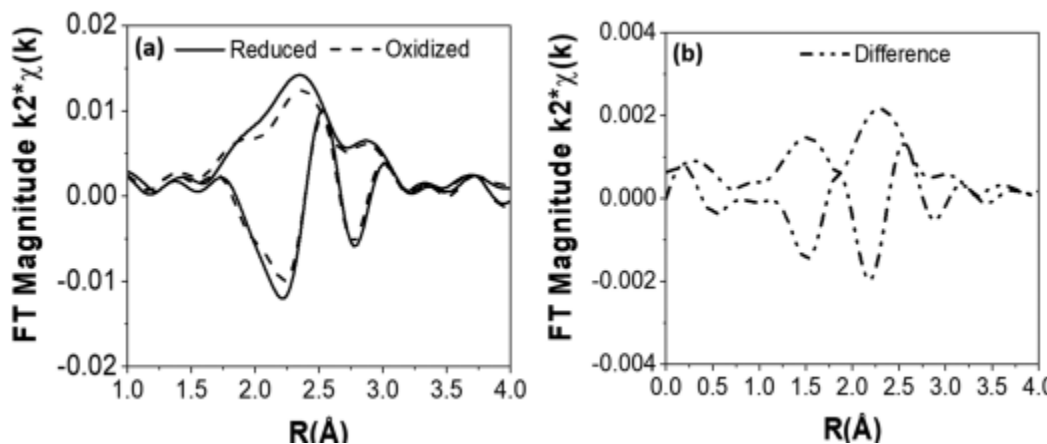
Case Study 1: Incomplete Formation of a Pt₃Cr Alloy



Approach for difference analysis, where reduced Pt-Cr nanoparticles are subsequently oxidized and the EXAFS (chi) data is subtracted to isolate the surface atoms

The **metallic bonds** of the **oxidized nanoparticles** are **identical** to those of the particle interior of the **reduced sample**, the difference spectrum represents the bonds only from the surface.

Case Study 1: Incomplete Formation of a Pt₃Cr Alloy



2Pt3Cr/SiO₂ after reduction at 550 °C: (a) Fourier transform magnitudes and imaginary components of the reduced and oxidized catalysts. (b) Difference EXAFS.

XRD of **2Pt-3Cr** -reduction at 550°C – Pt and Pt₃Cr phases ; 800 °C – bimetallic phase Pt₃Cr .

2Pt-1Cr reduced at 550°C, the XRD pattern and EXAFS CN_{Pt-Cr: Pt-Pt} ratio and bond distances - nearly identical to that of **2Pt-3Cr** indicating that both catalysts have very similar average structures.

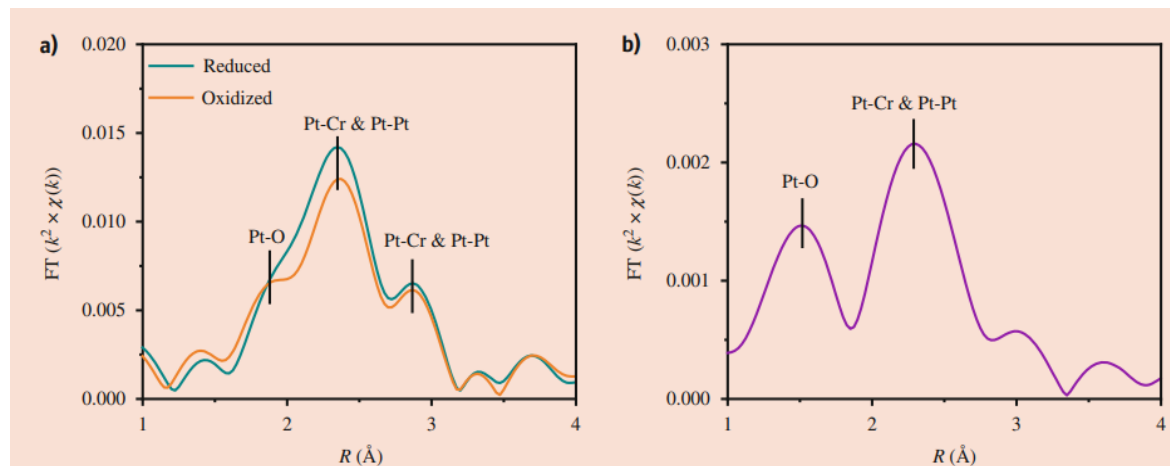
Both **2Pt-1Cr** and **2Pt-3Cr** form bimetallic catalysts with similar average compositions and structures, the differences in catalytic selectivity indicate that the surface compositions are not equivalent.

Case Study 1: Incomplete Formation of a Pt₃Cr Alloy



Table. Difference EXAFS fits for 2Pt-1Cr and 2Pt-3Cr

Catalyst	Scattering pair	CN	R (Å)
2Pt-1Cr	Pt-Pt	1.5	2.75
	Pt-Cr	0.6	2.71
	Pt-O	0.4	2.05
2Pt-3Cr	Pt-Pt	0.9	2.73
	Pt-Cr	0.5	2.73
	Pt-O	0.3	2.05



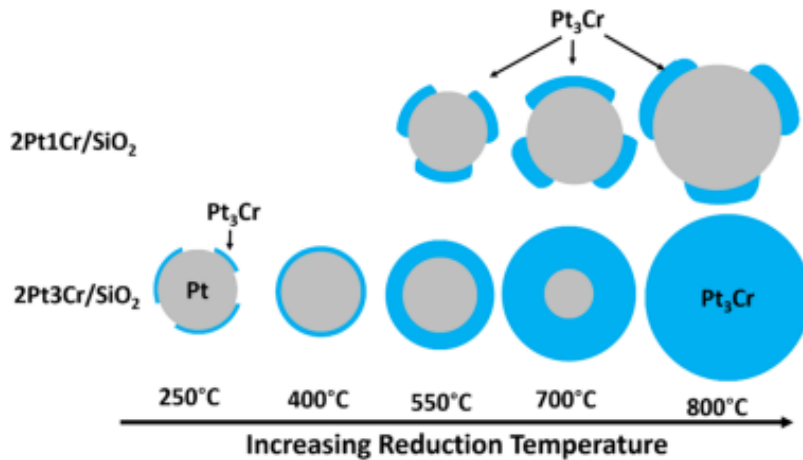
The k^2 -weighted Fourier transform of chi of 2Pt-3Cr after reduction at 550°C; (a) the reduced, oxidized, and (b) difference EXAFS



Case Study 1: Incomplete Formation of a Pt₃Cr Alloy

Table. EXAFS Coordination Ratios for the Reduced (Average), Oxidized (Particle Interior), and Difference (Surface) of Bimetallic Pt–Cr Nanoparticles

sample	reduction temperature (°C)	CN _{Pt–Cr} /CN _{Pt–Pt}		
		average	interior	surface
2Pt1Cr/SiO ₂	550	0.28	0.25	0.40
	700	0.35	0.31	0.40
	800	0.38		
2Pt3Cr/SiO ₂	250	0.16	0.11	0.31
	400	0.24	0.14	0.45
	550	0.30	0.22	0.56
	700	0.46	0.43	0.71
	800	0.52		



Cr incorporation into Pt nanoparticles in 2Pt1Cr/SiO₂ and 2Pt3Cr/SiO₂ with the increasing reduction temperature.

Summary

The average nanoparticle composition of two Pt–Cr alloy catalysts is similar, but their catalytic performance is not, and this difference is related to the surface composition.

A precise understanding of the surface structure in alloy nanoparticles, therefore, is critical for relating the active site structure to catalytic performance.



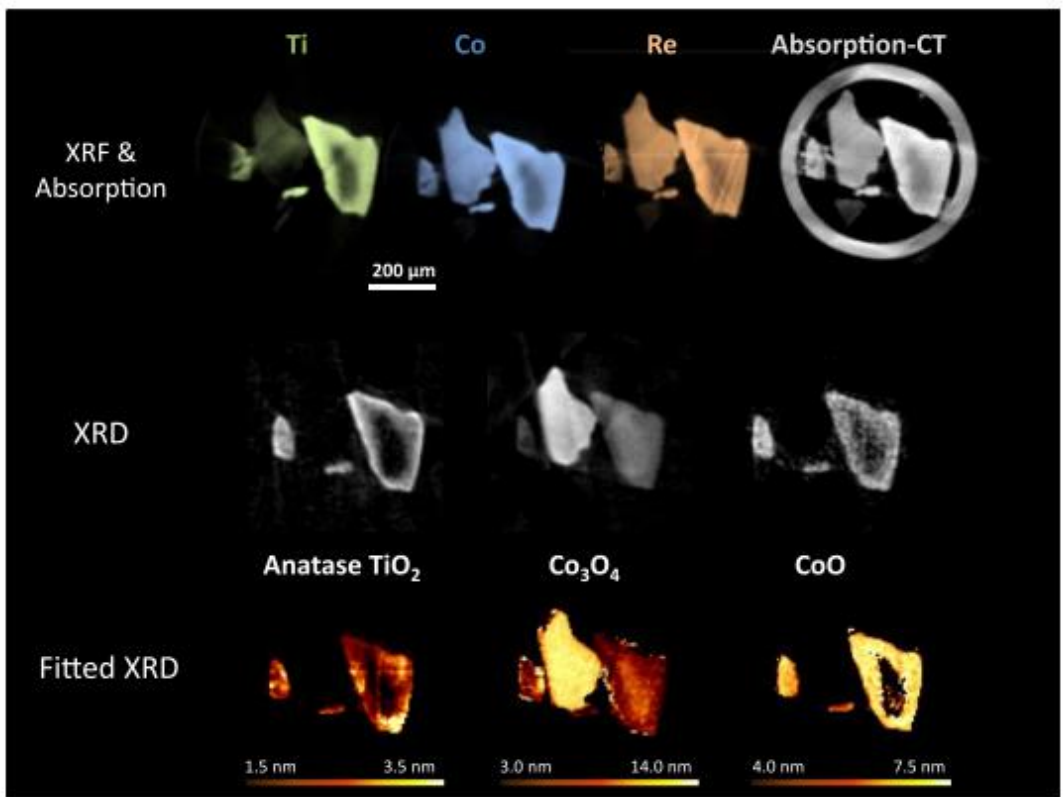
Case Study 2: Catalyst Preparation protocol

FTS Catalyst - consisting of 5% Ti/10% Co/1% Re on SiO_2

Five-dimensional (5D) color imaging

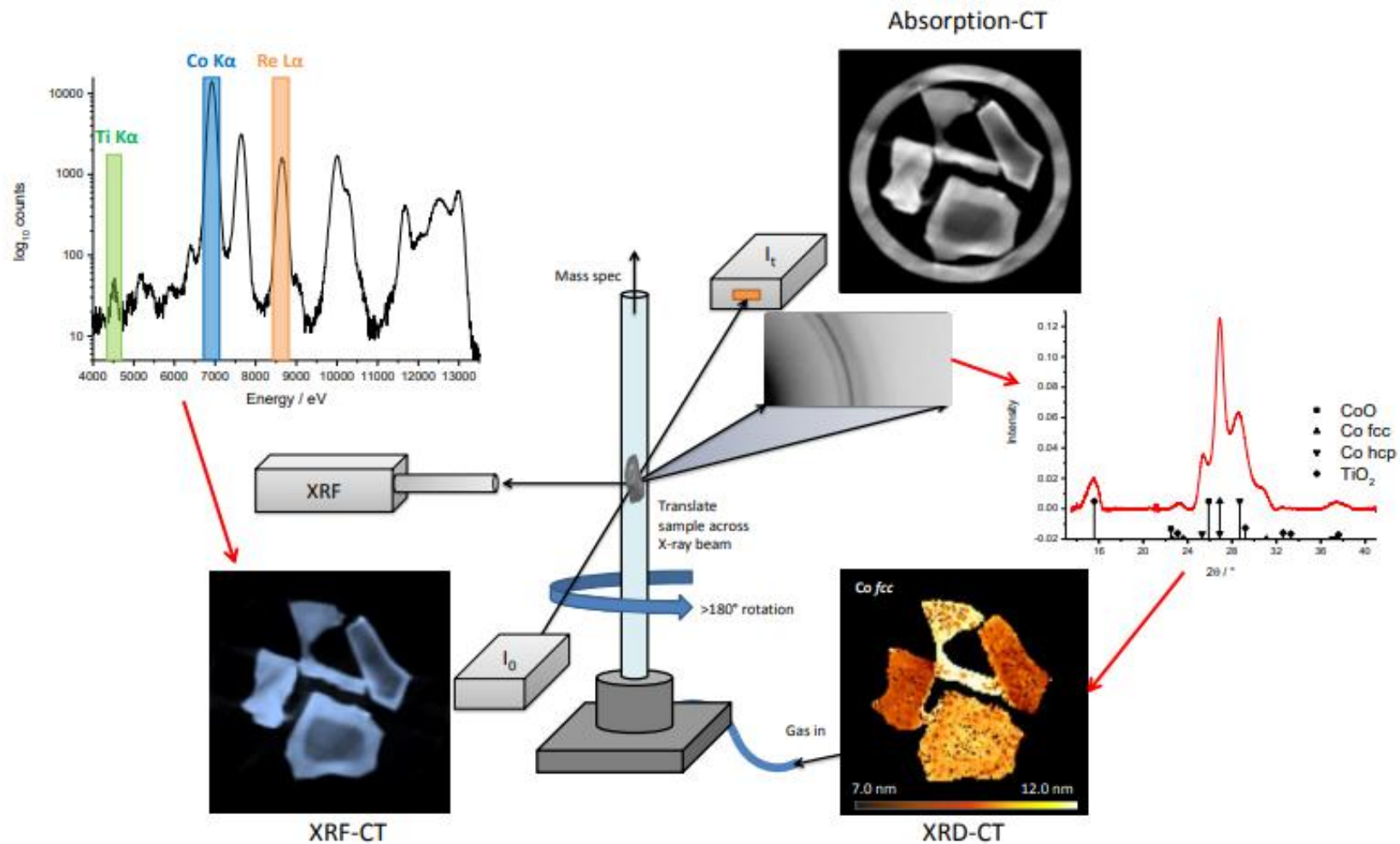
Operando multimodal imaging techniques like XRD-CT, XRF-CT, and absorption-contrast CT.

Different impregnation sequences yielded materials with the same chemical compositions, but the size and distribution of crystalline species were significantly altered.



Conventional catalyst precursor structure.

Case Study 2: Catalyst Preparation protocol



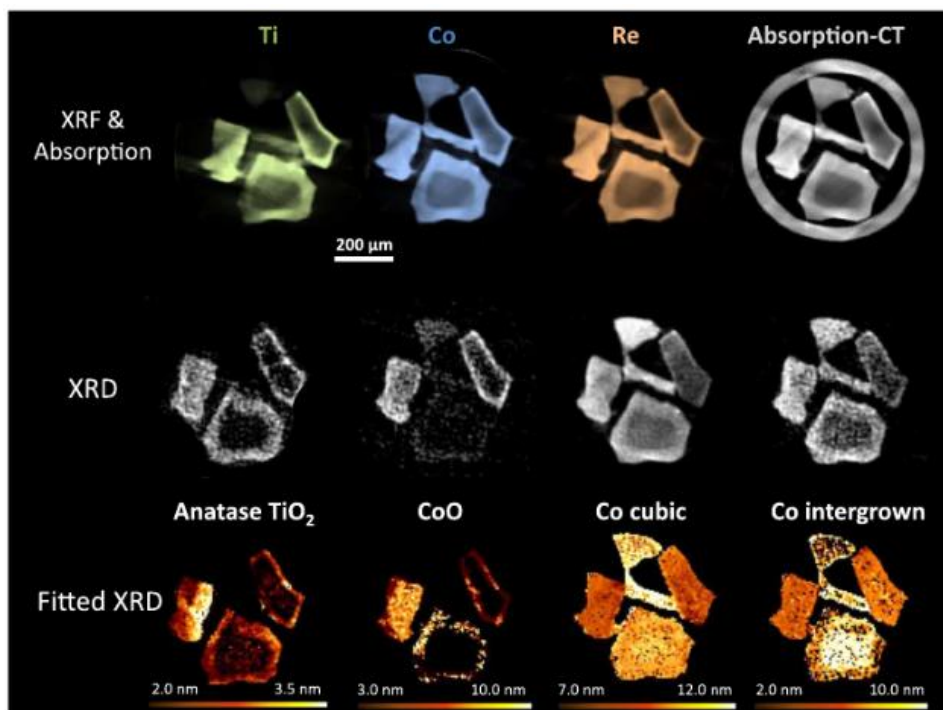
Schematic of the experimental setup including exemplar XRF spectrum and XRD pattern.

Case Study 2: Catalyst Preparation protocol



Conventional

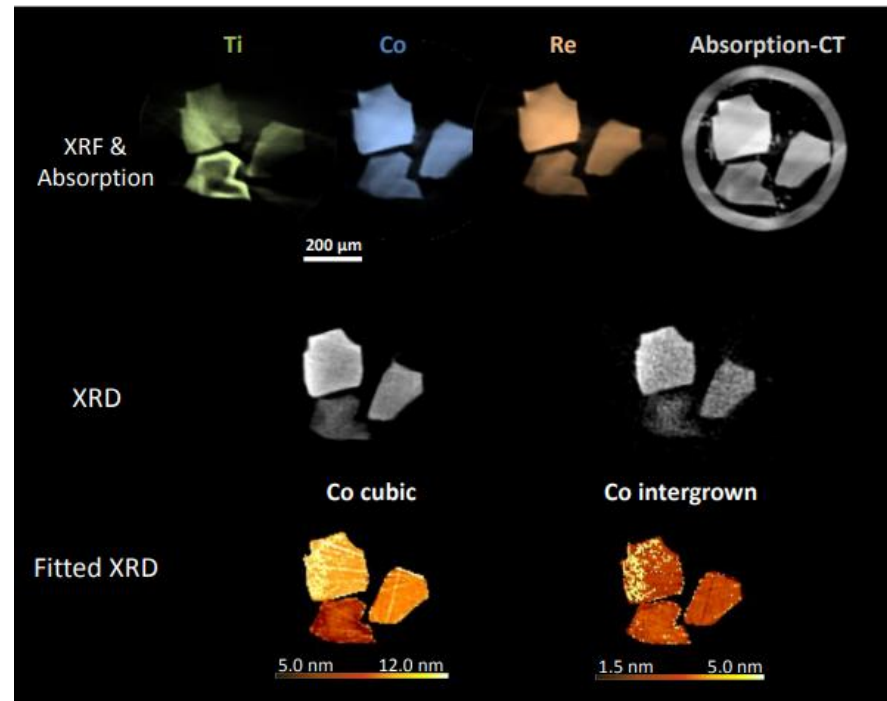
Suppressed the diffusion/migration of Co and Re species to the core of catalyst particles.



XRF-CT reconstructions showing elemental distributions for conventional catalyst structure during FTS at 4 bar.

Inverse configuration

Co and Re species freely diffused through the support material.



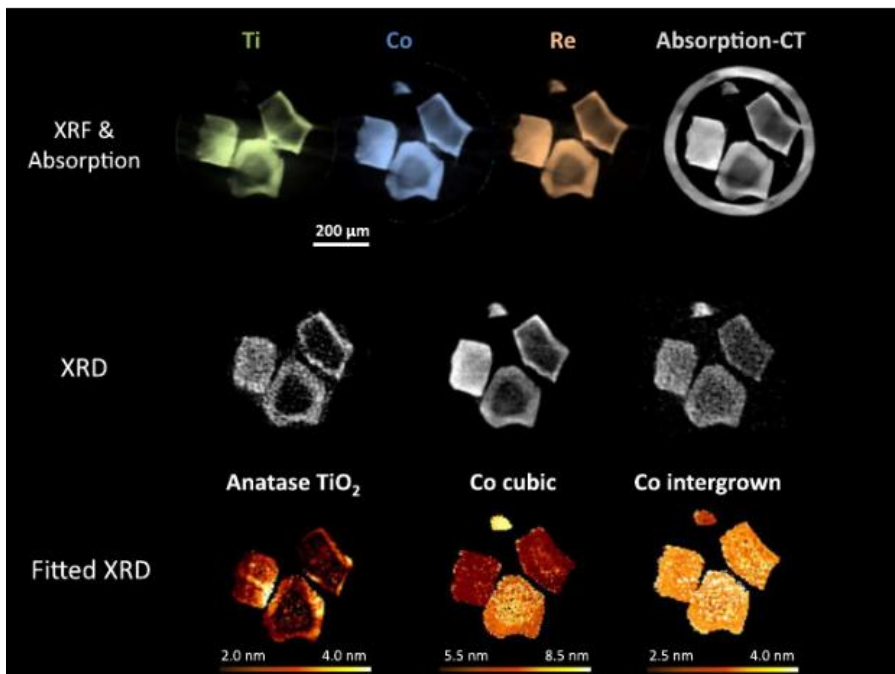
XRF-CT reconstructions showing elemental distributions for inverse catalyst during FTS at 4 bar.

Case Study 2: Catalyst Preparation protocol



Conventional

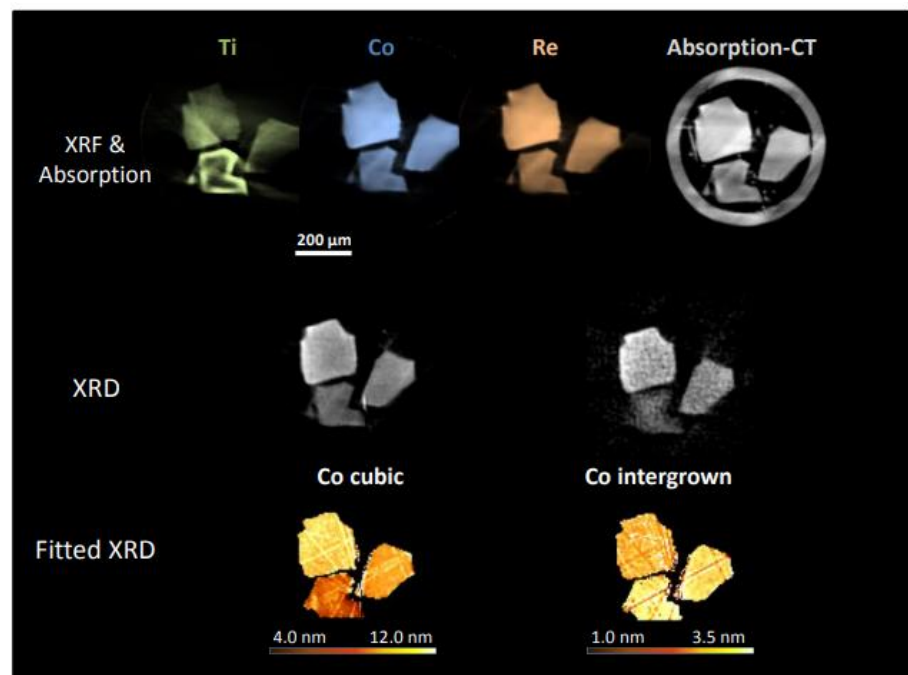
Reduced Co nanoparticles were smaller and more strained due to the *higher degree of intergrowth between hexagonal and cubic Co particles.*



Conventional catalyst structure after reduction

Inverse configuration

Formation of Larger Co Nanoparticles but *less strained, and the catalyst exhibited higher stability and selectivity for longer-chain hydrocarbons.*



Inverse catalyst structure after reduction

Case Study 2: Catalyst Preparation protocol



Summary

Small variations in the deposition sequence can result in catalysts with identical chemical composition, yet differ in spatial distribution of elements, different phases, and crystallite sizes, and, notably, in their activity and selectivity to specific products.

*Multimodal approach is used here to image the catalysts *operando*. Represent the first true simultaneous chemical tomography experiment.*

Conclusion

XAS is *element specific* and can *distinguish between different valences or coordination numbers* of an element within this specific range of energies.

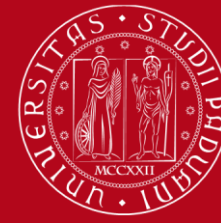
XAS therefore *enables the elucidation of how introduced species* change the (average) state of the catalyst.

In situ and *operando spectroscopy* offers the possibility to investigate *various aspects of such catalytic processes* in great detail as it is aimed at *characterization of catalysts in their active state*.

An in-depth understanding of *reaction* and *deactivation mechanisms* can lead to the *design of new and improved catalytic processes* in terms of *activity, selectivity, stability*, and as such can have major effects on sustainability and economic factors.

References

- Weckhuysen, B. M., Wondergem, C. S., & Vogt, C. (2023). Time-Resolved X-Ray Absorption Spectroscopy (XAS). In *Springer Handbook of Advanced Catalyst Characterization* (pp. 601-623). Cham: Springer International Publishing.
- Cutsail III, G. E., & DeBeer, S. (2022). Challenges and opportunities for applications of advanced X-ray spectroscopy in catalysis research. *ACS Catalysis*, 12(10), 5864-5886.
- Van Ravenhorst, I. K., Hoffman, A. S., Vogt, C., Boubnov, A., Patra, N., Oord, R., ... & Weckhuysen, B. M. (2021). On the cobalt carbide formation in a Co/TiO₂ Fischer–Tropsch synthesis catalyst as studied by high-pressure, long-term operando X-ray absorption and diffraction. *ACS catalysis*, 11(5), 2956-2967.
- Lin, S. C., Chang, C. C., Chiu, S. Y., Pai, H. T., Liao, T. Y., Hsu, C. S., ... & Chen, H. M. (2020). Operando time-resolved X-ray absorption spectroscopy reveals the chemical nature enabling highly selective CO₂ reduction. *Nature Communications*, 11(1), 3525.
- LiBretto, N. J., Yang, C., Ren, Y., Zhang, G., & Miller, J. T. (2019). Identification of surface structures in Pt₃Cr intermetallic nanocatalysts. *Chemistry of Materials*, 31(5), 1597-1609.
- Price, S.W.T., Martin, D.J., Parsons, A.D., Wojciech, A.S., Vamvakarios, A., Keylock, S.J., Beale, A.M., Mosselmans, J.F. W.: Chemical imaging of Fischer-Tropsch catalysts under operating conditions. *Sci. Adv.* 3, 1602838 (2017)
- Pascarelli, S. (2016, September). *Fundamentals of X-ray Absorption Fine Structure*. Presented at the Undergraduate Summer School, European Synchrotron Radiation Facility, Grenoble, France. [[link](#)]
- Mottana, A., & Marcelli, A. (2015). The historical development of X-ray Absorption Fine Spectroscopy and of its applications to Materials Science. *A Bridge between Conceptual Frameworks: Sciences, Society and Technology Studies* , 275-301.
- Newville, M. (2014). Fundamentals of XAFS. *Reviews in Mineralogy and Geochemistry*, 78(1), 33-74.
- Lytle, F. W. (1999). The EXAFS family tree: a personal history of the development of extended X-ray absorption fine structure. *Journal of Synchrotron Radiation*, 6(3), 123-134.



UNIVERSITÀ
DEGLI STUDI
DI PADOVA

Thank you